Nuclear fluid dynamics with long-mean-free path dissipation: Multipole vibrations and isoscalar giant resonance widths

Rainer W. Hasse*
Nuclear Science Division, Lawrence Berkeley Laboratory, Berkeley, California 94720 and Institut Laue-Langevin, F-38042 Grenoble, France

Gautam Ghosh
Sektion Physik, Universität München, D-8046 Garching, West Germany
(Received 16 February 1982)

The long-mean-free path nuclear fluid dynamics is extended to include damping. First the damping stress is derived from the solution of the Boltzmann equation for a breathing spherical container filled with a Fermi gas. Then the corresponding damping force is incorporated into Euler equations of motion and energies and widths of low lying collective resonances are computed as eigenfrequencies of a vibrating nucleus under surface tension and Coulomb potential as well as the high lying isoscalar giant resonances as eigenfrequencies of an elastic nucleus. Maximum damping is obtained if the particle frequency approximately resonates with the wall frequency. Theoretical results are compared with experimental data and future improvements are indicated.

[NUCLEAR STRUCTURE Nuclear giant resonances; calculated widths of isoscalar giant resonances. Elastic vibrations, Boltzmann equation, collision term, long-mean-free path dissipation.]

I. INTRODUCTION

Recently, the long outstanding problem of a macroscopic description of isoscalar giant resonance energies was solved. By performing a moment expansion of the Vlasov equation, Bertsch[1-3] derived elastic restoring forces against multipole deformations of a nucleus arising from a dynamic distortion of the Fermi sphere in the long-mean-free-path limit. The same result was obtained later on by Holzwarth[4-9] using the dynamical Thomas-Fermi approximation and by Wong[10,11] in evaluating the Bohm-Madelung quantum potential. The moment expansion of the Vlasov equation was then extended to higher moments by Winter.[12,13] Actual calculations of isoscalar giant resonance energies were performed with an approximate fluid velocity field,[14] also with inclusion of rotation,[15] or with exact solutions of the fluid dynamical equations.[16-19] It has been shown by the present authors[18] that due to the long-mean-free-path nature of nuclear dynamics, inclusion of higher than second moments of the Vlasov equation is essential in a realistic model, whereas in Ref. 19, these effects were simulated by introducing an effective mass. At present, even the most sophisticated macroscopic theory yields only reasonable agreement with experiment of 0^+, 1^-, 2^+, 3^- isoscalar giant resonance energies.

Concerning the widths of the giant resonances, a macroscopic description is far from being established. Although attempts to explain the widths as arising from ordinary two-body viscosity were quite successful,[14,19-23] they lack a physical basis. In particular, the elastic behavior mentioned above and viscosity have the same origin but emerge from opposite assumptions. As is well known in the theory of elasticity,[24] the stress tensor in the Euler equations of motion for vibrations of incompressible media has the form

$$\Sigma_{ij}=\frac{\mu}{i\omega+\tau^{-1}}\left[\frac{\partial u_i}{\partial x_i}+\frac{\partial u_j}{\partial x_i}\right]. \tag{1.1}$$

Here $\vec{u}$ is the fluid dynamical velocity, μ is the Lamé coefficient to the discussed below, ω is the frequency of oscillation, and τ is a mean free collision time which is proportional to the mean free path. In the limit of large τ, i.e., $\omega\tau\gg 1$, Eq. (1.1), hence, is the elastic stress tensor, whereas for small τ it represents the Navier-Stokes viscous stress ten-

sor with viscosity coefficient $\eta=\mu\tau$. A corresponding relation (1.1) holds in connection with nuclear vibrations.[12]

The one-body dissipation wall formula,[25] on the other hand, by its inherent assumption of a long mean free path,[26,27] provides a better basis for the damping mechanism of nuclear vibrations. Calculated giant resonance widths, however, are too large as compared with experimental data.[14,28] This is similar to results obtained in fission calculations including one-body dissipation, where the motion turned out to be overdamped. It seems to be due to the assumption of a solid wall in the derivation of the one-body dissipation formula[25] which allows for large irreversible density fluctuations in the vicinity of the surface.

This problem has been attacked in the theory of Winter,[12] where the Boltzmann equation is solved with a space dependent mean free collision time. As a result, τ^{-1} is peaked in the surface, and two-body collisions are concentrated in the nuclear surface. This explains nicely the origin of one-body dissipation on the basis of two-body collisions. A self-consistent solution of the corresponding Euler equations, however, is not available at present. As a first application, giant resonance widths were calculated in the harmonic oscillator basis.[29]

In this paper, we choose an intermediate way. We solve the Boltzmann equation with a collision term for monopole vibration with the approximation of $\tau\rightarrow\infty$ in the interior. In this way, particles are randomized in the interior and only collide with the wall which manifests itself in the boundary condition of specular reflection. This model is in the spirit of the theory of damping of Fermi liquids[30,31] simplified to a Fermi gas.[26,27,32] Having solved for the distribution function, we calculate the damping stress tensor which, then, is assumed to hold for all multipolarities of vibration.

Incorporating this damping stress into the Euler equations of motion, we solve them for the low-lying hydrodynamic modes and the high-lying elastic giant resonance modes. By virtue of the assumption of a nuclear Fermi gas, the model has no inherent adjustable parameters. However, in order to study the influence of this type of damping on nuclear vibrations, we vary the strength of the damping but compare with experimental data only those results obtained with the Fermi gas parameters. As a result, we find that damping is strongest if the particle frequency is approximately in resonance with the boundary frequency. Computed widths of the giant monopole resonance are too large as compared with experiments.

II. PISTON MODEL IN SPHERICAL GEOMETRY

A. Boltzmann equation

In this section we extend the one dimensional piston model of Ref. 27 to the spherical geometry. Let the solid wall of a spherical container with radius $R(t)$, filled with a (rarefied) Fermi gas, vibrate with normal velocity $\dot{R}=u_r\propto e^{i\omega t}$ and we solve the forceless Boltzmann equation

$$\left[\frac{\partial}{\partial t}+\frac{\vec{p}}{m}\cdot\vec{\nabla}\right]f=I[f] \tag{2.1}$$

for the distribution function $f(\vec{r},\vec{p},t)$. Here, $\vec{p}$ is the particle velocity and $I[f]$ is the collision integral. For a small departure from the zero temperature Fermi distribution we write

$$f=f_0+\delta f\ , \tag{2.2}$$

$$f_0=\frac{2}{h^3}\Theta(\epsilon_F-\epsilon)\Theta(R-r)\ , \tag{2.3}$$

where $\epsilon_F=p_F{}^2/2m=mv_F{}^2/2$ is the Fermi energy.

With this linearization the first order approximation to the collision integral reads[33] $I[f]\approx-\delta f/\tau$, where τ is the mean free collision time. Furthermore, in the radial geometry the Boltzmann equation reduces to

$$\left[\frac{\partial}{\partial t}+\frac{1}{\tau}+\frac{p}{m}\mu\frac{\partial}{\partial r}\right]\delta f=0\ . \tag{2.4}$$

Here $\mu=\cos\psi$, where ψ is the angle between momentum and radius vectors defined in such a way that $\mu>0$ ($\mu<0$) denotes particles heading towards the wall (the interior). The Pauli principle is implemented automatically if we only allow for scattering of particles at the Fermi energy,

$$\delta f=\frac{\partial f_0}{\partial\epsilon}\delta\epsilon\ , \tag{2.5}$$

$$\frac{\partial f_0}{\partial\epsilon}=-\frac{2}{h^3v_F}\delta(p_F-p)\Theta(R-r)\ . \tag{2.6}$$

This turns the Boltzmann equation into

$$\left[\frac{\partial}{\partial t}+\frac{1}{\tau}+v_F\mu\frac{\partial}{\partial r}\right]\delta\epsilon=0\ . \tag{2.7}$$

Equation (2.7) is only valid in the interior, $r<R$, where the mean free collision time is large. At the surface, Eq. (2.7) has to be solved with the boundary condition of specular reflection. The tangential component of the momentum is continuous whereas the radial component changes by $2mu_r\mu$

and the part of the change of energy linear in u_r is

$$\delta\epsilon(r=R)=-2mu_r v_F\mu \ . \tag{2.8}$$

The solution of Eq. (2.7) consistent with the boundary condition (2.8) is given by

$$\delta\epsilon=-2mv_F u_r\mu\Theta(-\mu) \times\exp\frac{(R-r)(i\omega+\tau^{-1})}{\mu v_F} \ . \tag{2.9}$$

Note that the step function $\Theta(-\mu)$ allows only for reflected particles being disturbed. Furthermore, the disturbance decays exponentially with $1/\lambda$, where $\lambda=v_F\tau$ is the mean free path. Since $R/\lambda\lesssim 1$ this decay is small and we can safely put τ, $\lambda\to\infty$ in the interior. On the other hand, the disturbance oscillates rapidly in the interior provided that

$$\frac{\omega R}{v_F}\gg 1 \ . \tag{2.10}$$

For a realistic soft wall, hence, the disturbance will be a superposition of many slightly phase shifted rapid oscillations, which approximately average out in the interior. As a consequence, the disturbance is peaked in the surface which is in the spirit of the one-body damping mechanism. As we shall see below, however, relation (2.10) is not well fulfilled for nuclear giant oscillations and the arguments given above hold only approximately.

$$E_n(x)=\int_0^1 d\mu\,\mu^{n-2}e^{-x/\mu}\to\begin{cases}\dfrac{1}{n-1}-\dfrac{x}{n-2}\ , & |x|\ll 1\\ e^{-x}/x\ , & |x|\gg 1\end{cases} \tag{2.15}$$

which obey the differential relation $E_n'=-E_{n-1}$. This yields the rate of energy dissipation

$$-\dot{E}=8\pi\rho_0\bar{v}R^2u_r{}^2E_3(0) \tag{2.16}$$

$$=\rho_0\bar{v}u_r{}^2S \ , \tag{2.17}$$

where $S=4\pi R^2$ is the surface area. Equation (2.17) is the one-body dissipation formula[25] for constant surface velocity which is obtained here for a solid vibrating container in approximation (2.10).

Evaluation of the damping stress tensor proceeds in a similar way. Let

$$u_i=\langle p_i/m\rangle \tag{2.18}$$

be the component of the fluid velocity and

$$P_{ij}=\langle p_ip_j/m\rangle-mu_iu_j \tag{2.19}$$

be the total pressure tensor, where averages are performed with the total distribution function f. It splits up into the static Fermi gas pressure and the damping stress tensor[34]

$$P_{ij}=\tfrac{1}{5}\rho_0v_F\delta_{ij}-\Sigma_{ij} \ , \tag{2.20}$$

$$\Sigma_{ij}=-\frac{1}{m}\int d^3p\,p_ip_j\delta f =-\frac{3\rho_0u_r}{mp_F{}^3}\int dp\,p^2\delta(p_F-p) \times\int_{-1}^0 d\mu\,p_ip_j\mu\Theta(-\mu)e^{\xi/\mu} \ . \tag{2.21}$$

The last integral is confined to the half space with

$$\frac{\pi}{2}\le\psi\le\frac{3\pi}{2} \ ;$$

see Fig. 1. We therefore express the momentum components with polar angles θ, φ in terms of the angle ψ by two successive rotations. First rotate $\vec{r}$

B. Energy loss and damping stress

We now proceed to calculate the rate of energy loss and the damping stress tensor associated with the disturbance (2.9). The change in energy due to a change in radius δR under the assumption (2.10) is

$$\delta E=\int d^3p\frac{p^2}{2m}\int_R^{R+\delta R}d^3r\,\delta f =8\pi\rho_0\bar{v}u_r\int_R^{R+\delta R}dr\,r^2\int_{-1}^0 d\mu\,\mu e^{\xi/\mu} \ . \tag{2.11}$$

Here we used the abbreviation

$$\xi=\frac{(R-r)(i\omega+\tau^{-1})}{v_F} \ , \tag{2.12}$$

the Fermi gas density ρ_0, and average particle velocity $\bar{v}=\langle p/m\rangle$,

$$\rho_0=\frac{8\pi mp_F{}^3}{3h^3} \ , \tag{2.13}$$

$$\bar{v}=\tfrac{3}{4}v_F \ . \tag{2.14}$$

The latter integral is evaluated in terms of the exponential integrals

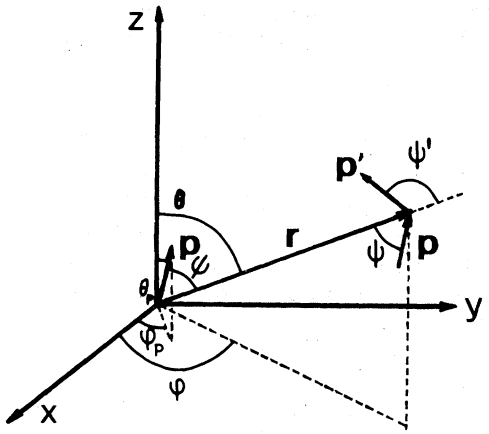

FIG. 1. Vectors and angles employed in the piston model.

and $\vec{p}$ about the z axis by an angle $-[(\pi/2)+\varphi]$. The vector $\vec{r}$ lies now in the y-z plane. Then rotate $\vec{r}$ by an angle θ about the x axis. The vector $\vec{r}$ is now along the z axis and the vector $\vec{p}$ goes over to $\vec{p}\,'$ with

$$\begin{pmatrix} p_x \\ p_y \\ p_z \end{pmatrix} = \begin{pmatrix} -\sin\varphi & -\cos\varphi & 0 \\ \cos\varphi & -\sin\varphi & 0 \\ 0 & 0 & 1 \end{pmatrix} \begin{pmatrix} 1 & 0 & 0 \\ 0 & \cos\theta & -\sin\theta \\ 0 & \sin\theta & \cos\theta \end{pmatrix} \begin{pmatrix} p_x' \\ p_y' \\ p_z' \end{pmatrix} . \tag{2.22}$$

The polar angle of $\vec{p}\,'$ is now ψ and the integral becomes

$$\Sigma_{ij} = 2\rho_0 \bar{v} u_r \left[\left(\tfrac{5}{3} E_3(\xi) - 3E_5(\xi)\right)\delta_{ij} + \left(3E_5(\xi) - E_3(\xi)\right)\frac{x_i x_j}{r^2} \right] . \tag{2.23}$$

Close to the surface, by use of (2.15), Eq. (2.23) simplifies to

$$\Sigma_{ij} = \tfrac{1}{2}\rho_0 \bar{v} u_r \left[\delta_{ij} + \frac{x_i x_j}{r^2} \right] . \tag{2.24}$$

In spherical coordinates, there are only diagonal components of the stress tensor,

$$\begin{aligned} &\Sigma_{rr} = 2\Sigma_{\theta\theta} = 2\Sigma_{\varphi\varphi} = \rho_0 \bar{v} u_r , \\ &\Sigma_{r\theta} = \Sigma_{r\varphi} = \Sigma_{\theta\varphi} = 0 , \end{aligned} \tag{2.25}$$

As a result, the damping mechanism produces an isotropic pressure $-\frac{1}{2}\rho_0 \bar{v} u_r$ and an additional radial-radial stress $\frac{1}{2}\rho_0 \bar{v} u_r$ and, hence, a damping force $\vec{F} = \vec{\nabla}\cdot\vec{\Sigma}$ on the rhs of the Euler equation of motion,

$$\vec{F} = \tfrac{1}{2}\rho_0 \bar{v} (\vec{\nabla} u_r + \vec{e}_r \vec{\nabla}\cdot(u_r \vec{e}_r)) . \tag{2.26}$$

Although (2.25) has been derived in the vicinity of the surface only, we employ (2.25) and (2.26) all over the nuclear volume. This is a safe approximation since, as will be shown below, u_r is small in the interior. For a freely vibrating surface, the rate of energy dissipation induced by an arbitrary stress tensor Σ is given by

$$-\dot{E} = \int d^3 r \, \vec{\vec{\Sigma}} \vec{\nabla}\cdot\vec{u} . \tag{2.27}$$

With the damping stress (2.24) or (2.25) it attains the form

$$-\dot{E} = \tfrac{1}{2}\rho_0 \bar{v} \int d^3 r \left[u_r \vec{\nabla}\cdot\vec{u} + \frac{1}{2}\frac{\partial u_r^2}{\partial r} \right] . \tag{2.28}$$

Here, the first part is due to compression caused by the isotropic damping pressure and the second part arises from the additional radial-radial stress.

C. Rough estimate

As a first simple application we compare the rate of energy dissipation in our theory during a multipole vibration,

$$R(\theta,\varphi) = R_0(1+\alpha_l Y_{l0}(\theta)) , \tag{2.29}$$

with the one obtained by using the one-body dissipation formula, thereby employing potential flow, $\vec{\nabla}\cdot\vec{u} = 0$,

$$u_r = R_0^{2-l} \dot{\alpha}_l r^{l-1} Y_{l0}(\theta) , \tag{2.30}$$

as a first estimate for the fluid velocity. From (2.28) we get

$$-\dot{E} = \tfrac{1}{4}\rho_0 \bar{v} R_0{}^4 \dot{\alpha}_l{}^2 \frac{l-1}{l} , \tag{2.31}$$

whereas the one-body dissipation formula yields

$$-\dot{E}_{\text{one body}} = \rho_0 \bar{v} R_0{}^4 \dot{\alpha}_l{}^2 . \tag{2.32}$$

Thus damping of vibrations of large multipole numbers with the present mechanism is about one fourth as weak as compared to the one-body mechanism. This is due to the fact that solenoidal flow actually is not compatible with the assumption of a solid surface. Furthermore, for low multipole numbers, our damping is even smaller by another factor of $(l-1)/l$. It also has the desired feature that pure translational motion is not damped, the

lack of this being an inherent deficiency of the original one-body dissipation formula.

III. DISSIPATIVE HYDRODYNAMICS

Low-lying hydrodynamic vibrations result from an interplay between Coulomb and surface energy restoring forces.[35] Apart from shell and deformation effects, they should approximately obey an $A^{-1/2}$ dependence. Experimental identification of these states, however, is still speculative. In this section we solve the Euler equations of motion with surface and Coulomb energies and damping stress exactly. Although the mean particle velocity $\bar{v}=0.205c$, which is the analog to the viscosity constant in our theory for a Fermi gas is a natural constant, we will treat it as a free parameter and study the influence of its strength on the results.

In this terminology, the linearized Euler equations of motion read

$$\rho_0\dot{\vec{u}}+\vec{\nabla}(\delta p+\rho_0\delta\phi_C)=\tfrac{1}{2}\rho_0\bar{v}(\vec{\nabla}u_r+\vec{e}_r\vec{\nabla}\cdot(u_r\vec{e}_r)) , \tag{3.1}$$

where δp and $\delta\phi_C$ are the deviations of the pressure and Coulomb potential from their respective spherical values. For damped harmonic motion, $\vec{u}\propto e^{i\Omega_l t}$, the ansatzes

$$u_r=V(r)Y_{l0} , \tag{3.2a}$$

$$u_\theta=W(r)\frac{\partial Y_{l0}}{\partial\theta} , \tag{3.2b}$$

$$\frac{\delta p}{\rho_0}+\delta\phi_C-\tfrac{1}{2}\bar{v}u_r=\Psi(r)Y_{l0} , \tag{3.2c}$$

and the incompressibility assumption $\vec{\nabla}\cdot\vec{u}=0$ satisfy (3.1) and yield

$$\Psi=-i\Omega_l rW=-\frac{i\Omega_l}{l(l+1)}\frac{d}{dr}(r^2V) \tag{3.3}$$

and the second order differential equation

$$\frac{d^2V}{dr^2}+\left[\frac{4}{r}+\frac{l(l+1)\bar{v}}{2i\Omega_l r^2}\right]\frac{dV}{dr}+\left[\frac{2-l(l+1)}{r^2}+\frac{l(l+1)\bar{v}}{i\Omega_l r^3}\right]V=0 . \tag{3.4}$$

In terms of the variable

$$y=\frac{il(l+1)\bar{v}}{2\Omega_l r} , \tag{3.5}$$

the solution regular at the origin is a hypergeometric function which can be written explicitly,

$$V(y)=C_l y^{1-l}e^{-y}L_{l-1}^{(-2l-1)}(y) . \tag{3.6}$$

Here $L_{l-1}^{(-2l-1)}(y)$ is the associated Laguerre polynomial of negative degree,

$$\begin{aligned} L_0^{(-3)}&=1 ,\\ L_1^{(-5)}&=-(y+4) ,\\ L_2^{(-7)}&=\tfrac{1}{2}(y^2+10y+30) . \end{aligned} \tag{3.7}$$

The normalization constant C_l is determined by Neumann's boundary condition which states that the fluid velocity at the boundary is equal to the boundary velocity,

$$u_r=R_0\dot{\alpha}_l Y_{l0} \tag{3.8}$$

and the complex eigenfrequency follows from Laplace's boundary condition

$$\Sigma_{rr}-p+\sigma\kappa=0, \quad r=R_0 . \tag{3.9}$$

Here, σ is the surface tension and κ the Gaussian curvature. In principle, the tangential boundary condition

$$\Sigma_{r\theta}=0 \tag{3.10}$$

must also be fulfilled. However, by the very nature of the damping [see Eq. (2.25)] this condition is a trivial one. Equation (3.9) is evaluated with help of the surface quantities[21]

$$\begin{aligned} \Sigma_{rr}&=\frac{i}{2}\bar{v}\rho_0R_0\Omega_l\alpha_l Y_{l0} ,\\ \delta\phi_C&=\frac{4\pi R_0{}^2\rho_e{}^2}{\rho_0(2l+1)}\alpha_l Y_{l0} ,\\ \kappa&=\frac{2}{R_0}+\frac{(l-1)(l+2)}{R_0}\alpha_l Y_{l0} ,\\ p&=\frac{2\sigma}{R_0}+\tfrac{4}{3}\pi R_0{}^2\rho_e{}^2\alpha_l Y_{l0} , \end{aligned} \tag{3.11}$$

and with the pure liquid drop eigenfrequency

$$\bar{\omega}_l=\left[\frac{l(l-1)(l+2)\sigma}{\rho_0R_0{}^3}-\frac{8\pi l(l-1)\rho_e{}^2}{3(2l+1)\rho_0}\right]^{1/2} . \tag{3.12}$$

In (3.11) and (3.12), ρ_e is the nuclear charge density. This yields the characteristic equation

$$\left[\frac{y_l}{l(l+1)\eta_l}\right]^2+1-\frac{y_l}{l+1}\frac{d}{dy_l}\ln L_{l-1}^{(-2l-1)}(y_l)=0 , \tag{3.13}$$

where

$$y_l=\frac{il(l+1)\bar{v}}{2\Omega_l R_0}$$

is related to the eigenfrequency, and

$$\eta_l=\frac{\bar{v}}{2R_0\bar{\omega}_l}$$
$$\approx\frac{\text{average particle frequency}}{\text{liquid drop wall frequency}} \tag{3.14}$$

is a dimensionless parameter.

Equation (3.13) is an algebraic equation in y_l of degree $(l+1)$. For dipole motion, it has only the trival solution $\Omega_1=\bar{\omega}_1=0$. For arbitrary multipole moments but small damping, $\eta_l\ll 1$, we get

$$\frac{\Omega_l}{\bar{\omega}_l}=1+i\frac{l-1}{8}\eta_l\ , \tag{3.15}$$

and for large damping, $\eta_l\gg 1$,

$$\frac{\Omega_l}{\bar{\omega}_l}=\left[\frac{l+1}{2}\right]^{1/2}+i\frac{(l-1)(l+2)}{8l\eta_l}\ . \tag{3.16}$$

The latter limit exhibits the interesting feature that there are no overdamped solutions and that damping becomes smaller again with a large damping constant. Numerical results of the complex eigenfrequency

$$\Omega_l=\omega_l+i\gamma_l \tag{3.17}$$

are displayed in Fig. 2. The damping width shows a strong resonance behavior about $\eta_l\approx 1$. According to Eq. (3.14), at this point the average particle frequency $\bar{v}/2R_0$ resonates with the liquid drop wall frequency $\bar{\omega}_l$, the latter being approximately equal to the actual wall frequency ω_l. This feature persists up to high multipole moments. For $l\gg 1$, evaluation of the characteristic equation (3.13) reveals that the maximum of γ_l lies at

$$\frac{\bar{v}}{R_0}=\omega_l=\gamma_l=\frac{1}{2}\left[\frac{l}{2}\right]^{1/2}\bar{\omega}_l\ , \tag{3.18}$$

which states that maximum damping is achieved if the average particle frequency resonates with the actual wall frequency.

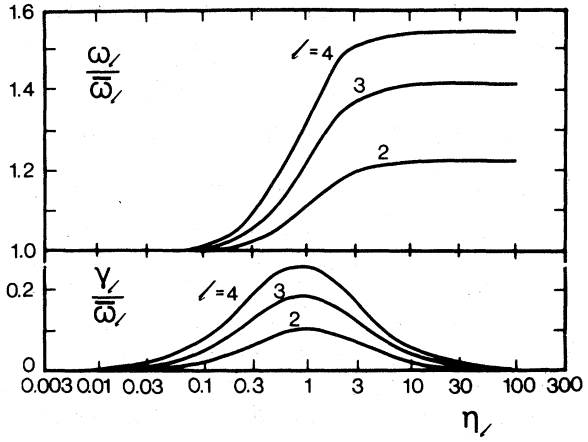

FIG. 2. Real (upper part) and imaginary (lower part) parts of the complex hydrodynamical eigenfrequency of multipolarity l in units of the pure liquid drop frequency. The variable η_l is the ratio of particle frequency to liquid drop wall frequency.

At this stage it is worth looking at the radial velocity component. Rewriting (3.6) yields

$$u_r=R_0\dot{\alpha}_l Y_{l0}\frac{\sum_{\nu=0}^{l-1}a_{l-1-\nu}\left[\frac{2\Omega_l r}{i\bar{v}l(l+1)}\right]^{\nu}}{\sum_{\nu=0}^{l-1}a_{l-1-\nu}\left[\frac{2\Omega_l R_0}{i\bar{v}l(l+1)}\right]^{\nu}}$$
$$\times\exp\left[\frac{\bar{v}l(l+1)}{2i\Omega_l}\left[\frac{1}{r}-\frac{1}{R_0}\right]\right]\ , \tag{3.19}$$

where a_ν are the coefficients of the Laguerre polynomial. For small damping, only the terms with $\nu=l-1$ are relevant and the exponential is approximately unity except for the point $r=0$, where it vanishes. This is the limit of potential flow, Eq. (2.30). For large damping, on the other hand, only the terms with $\nu=0$ are relevant. From (3.16) we then obtain

$$u_r=R_0\dot{\alpha}_l Y_{l0}\exp\left[-\frac{(l-1)(l+2)}{4}\left[\frac{R_0}{r}-1\right]-i\eta_l l[2(l+1)]^{1/2}\left[\frac{R_0}{r}-1\right]\right]\ . \tag{3.20}$$

It decays and strongly oscillates in the interior of the nucleus, the higher the multipolarity is, the stronger, which are exactly those features which we concluded above from the solution of the Boltzmann equation. Furthermore, this implicitly justifies the assumption (2.24) of extending the surface stress tensor into the interior region.

For the computation of η_l values from (3.12) and (3.14) we employ the Fermi gas value for $\bar{v}$ and the ap-

proximation of $N=Z=A/2$. This yields

$$\eta_l \approx 3.35 x_F^{1/6} \left[\frac{2l+1}{l(l-1)[(l+2)(2l+1)-20x_F]} \right]^{1/2} , \tag{3.21}$$

where

$$x_F \approx A/200 \tag{3.22}$$

is the fissility. This quantity is plotted in Fig. 3. One sees that for quadrupole vibration, heavy nuclei lie beyond maximum damping in Fig. 1, whereas for higher multipole moments, they lie slightly in front of the maximum. In Fig. 4, energies $E_l=\hbar\omega_l$ and widths $\Gamma_l=2\hbar\gamma_l$ of the low hydrodynamic isoscalar vibrations are plotted. Although the interpretation of the experimental data of Refs. 36 and 37 in these terms is speculative, we observe rather good agreement for the octupole data. Unfortunately, there were no widths extracted from the data. The theoretical order of magnitude, $\Gamma_2 \approx 2$ MeV for medium heavy nuclei, however, is compatible with the experiments.

IV. DISSIPATIVE FLUID DYNAMICS

As outlined in the Introduction, the high lying isoscalar giant resonances in the long-mean-free-path approximation with neglection of higher moments of the Boltzmann equation are governed by the elastic equations of harmonic motion.[16–18] Including the long-mean-free-path damping force, they read

$$\rho_0 \ddot{\vec{u}} + \frac{i}{\Omega_l}((\lambda+2\mu)\vec{\nabla}\vec{\nabla}\times\vec{u} - \mu\vec{\nabla}\times\vec{\nabla}\times\vec{u}) = \tfrac{1}{2}\rho_0 \bar{v}(\vec{\nabla}u_r + \vec{e}_r\vec{\nabla}\cdot(u_r\vec{e}_r)) , \tag{4.1}$$

where

$$\mu/\rho_0 = \tfrac{1}{5}v_F^2 = (0.122c)^2 , \tag{4.2a}$$

$$\lambda = \frac{K}{gm} - \tfrac{2}{3}\mu , \tag{4.2b}$$

are the Lamé coefficients and K is the nuclear compressibility. In dealing with the 0^+ breathing mode, we shall employ the surface dependent compressibility

$$K = (300 - 600A^{-1/3}) \text{ MeV} . \tag{4.3}$$

whereas for the vibrational modes 2^+, 3^-, 4^+, and for the squeezing mode 1^-, it suffices to use the Poisson condition $K=15m\mu$, i.e.,

$$\lambda = \mu . \tag{4.4}$$

By making the same ansatzes (3.2a) and (3.2b) for the velocity components as above, the radial and tangential differential equations become

$$\Omega_l^2 V + \frac{\mu}{\rho_0}\left[\alpha\frac{d}{dr}\frac{1}{r^2}\frac{d}{dr}r^2V - l(l+1)\left[\frac{V}{r^2}+\alpha\frac{d}{dr}rW - \frac{1}{r^2}\frac{d}{dr}rW\right]\right] + i\frac{\bar{v}}{2}\Omega_l\left[\frac{1}{r^2}\frac{d}{dr}r^2V + \frac{dV}{dr}\right] = 0 , \tag{4.5a}$$

$$\Omega_l^2 W + \frac{\mu}{\rho_0}\left[\frac{1}{r}\frac{d^2}{dr^2}rW - \alpha l(l+1)\frac{W}{r^2} - \frac{1}{r}\frac{dV}{dr} + \frac{\alpha}{r^3}\frac{d}{dr}r^2V\right] + i\frac{\bar{v}}{2}\Omega_l\frac{dV}{dr} = 0 . \tag{4.5b}$$

Here,

$$\alpha = 2 + \frac{\lambda}{\mu} = \begin{cases} 3 , & 1^-,2^+,3^-,4^+,\ldots , \\ 3.727 - 4.787A^{-1/3} , & 0^+ \end{cases} \tag{4.6}$$

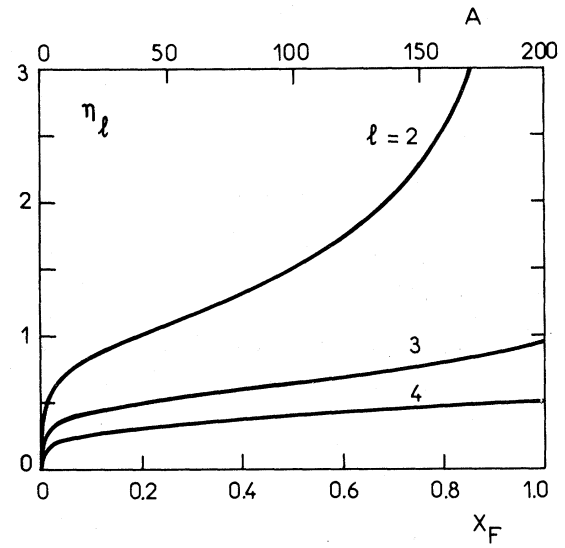

FIG. 3. The variable η_l plotted vs the nuclear fissility x_F or mass number A.

follows from (4.3) or (4.4), respectively. Equations (4.5) are augmented by the boundary conditions $\Sigma_{rr}=\Sigma_{r\theta}=0$ at the surface $r=R_0$,

$$2\frac{dV}{dr}+\frac{1}{r^2}\frac{d}{dr}r^2V-l(l+1)\frac{W}{r^2}+i\frac{\bar{v}\rho_0\Omega_l}{\mu}V=0\,, \tag{4.7a}$$

$$V+r\frac{dW}{dr}-W=0\,, \tag{4.7b}$$

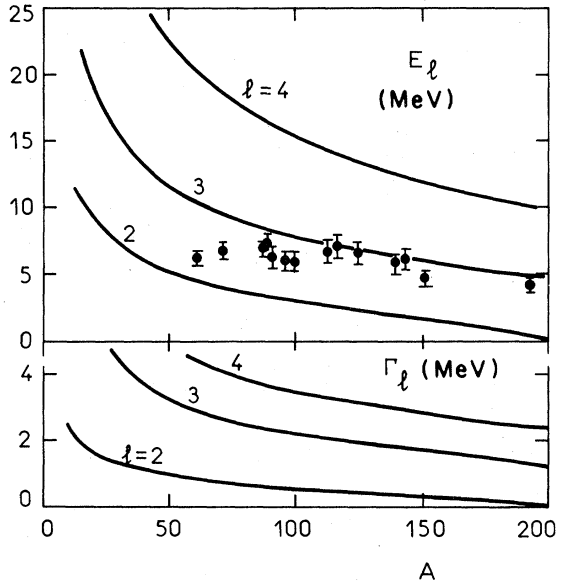

FIG. 4. Theoretical energies and widths of the low-lying hydrodynamical modes and experimental data (Refs. 36 and 37) of the energies of low-lying collective octupole resonances.

by the Neumann boundary condition at $r=R_0$,

$$V=R_0\dot{\alpha}\,, \tag{4.8}$$

and by the condition that V and W must vanish at the origin. In what follows, we shall employ the dimensionless damping constant

$$\eta=\frac{\bar{v}}{2}\left[\frac{\rho_0}{\mu}\right]^{1/2}=\frac{3\sqrt{5}}{8}=0.8385\,, \tag{4.9}$$

but vary its strength as we did above.

A. The monopole

Equations (4.5) can be solved for monopole vibrations, $l=0$. The tangential velocity component vanishes, $W=0$, and the radial velocity in terms of the dimensionless coordinate and frequency

$$x=r\Omega_0(\rho_0/\mu)^{1/2}\,, \tag{4.10a}$$

$$x_0=R_0\Omega_0(\rho_0/\mu)^{1/2}\,, \tag{4.10b}$$

reads

$$V(x)=\frac{\dot{\alpha}_0R_0}{j_1(\nu x_0)}e^{-i\eta x/\alpha}j_1(\nu x)\,, \tag{4.11}$$

where

$$\nu=\left[\frac{1}{\alpha}+\left[\frac{\eta}{\alpha}\right]^2\right]^{1/2}. \tag{4.12}$$

From the boundary condition (4.7a) we get the

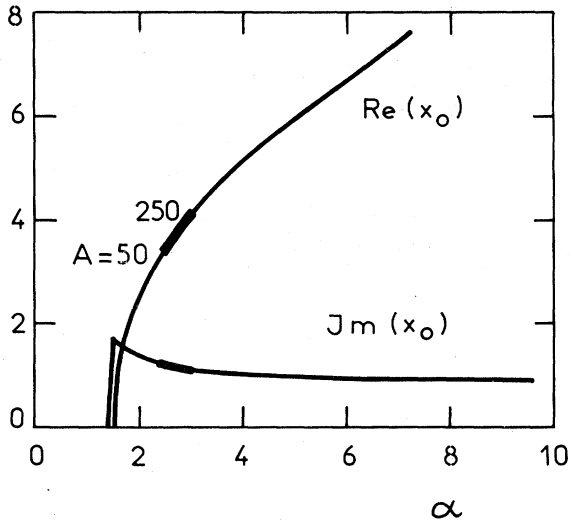

FIG. 5. Real and imaginary parts of the dimensionless complex monopole eigenfrequency vs the parameter α. Heavy portions indicate the location of nuclei.

characteristic equation for the complex eigenfrequency,

$$\alpha\nu j_0(\nu x_0)+(i\eta-4)j_1(\nu x_0)=0\ . \tag{4.13}$$

Here and in the following, energy and width of a giant resonance of multipolarity l with the Fermi gas parameters are given in terms of the complex solution x_l by

$$\begin{aligned} E_l&=\hbar\,\mathrm{Re}(\Omega_l)\\ &=20.452A^{-1/3}\ \mathrm{MeV}\,\mathrm{Re}(x_l)\\ \Gamma_l&=2\hbar\,\mathrm{Im}(\Omega_l)\\ &=40.904A^{-1/3}\ \mathrm{MeV}\,\mathrm{Im}(x_l)\ . \end{aligned} \tag{4.14}$$

The monopole solution is plotted in Fig. 5 against the parameter α. For the range of nuclei indicated, one observes a rather constant behavior of the imaginary part, thus giving rise to a well pronounced $A^{-1/3}$ dependence of the damping width. The real part, however, is increasing with increasing mass number which translates into a strong departure of the energy from the $A^{-1/3}$ law. For fixed $\alpha=3$, the dependence of the complex solution on the damping parameter is shown in the $l=0$ part of Fig. 6. Apart from the fact that for overdamped motion ($\eta>7.76$) there does not exist a creeping mode; the behavior is similar to the one resulting from ordinary two-body viscosity. Energies and widths are shown in Fig. 7 in units of $A^{-1/3}$ MeV or MeV,

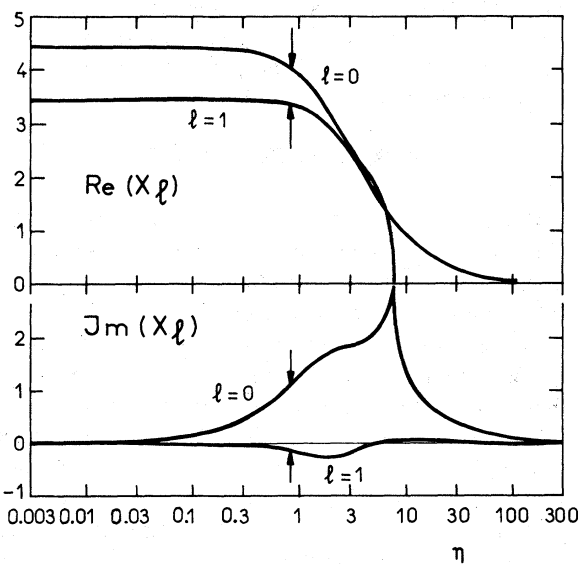

FIG. 6. Real and imaginary parts of the dimensionless monopole (breathing) and isoscalar dipole (squeezing) complex eigenfrequencies vs the damping parameter η. Arrows point to the Fermi gas values.

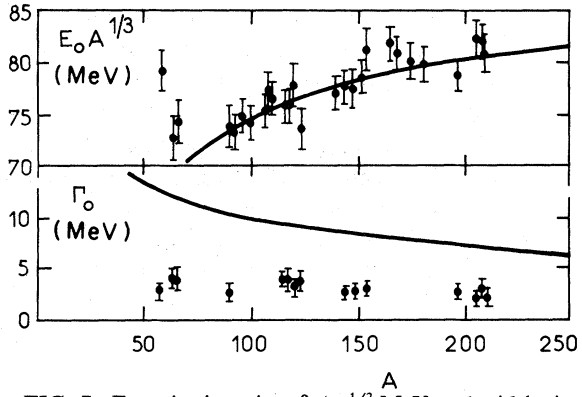

FIG. 7. Energies in units of $A^{-1/3}$ MeV and widths in units of MeV of the breathing mode compared with experimental data (Refs. 38 and 39).

respectively, together with experimental data taken from reviews.[38,39] Theoretical widths are roughly twice as large as the experiments. Note, however, that identification of the breathing modes for light nuclei $A\lesssim 80$ is still difficult by virtue of the fact that only approximately 50% of the sum rule is exhausted.[38]

B. Squeezing and vibrational modes

Owing to the fact that the monopole solution of the damped fluid dynamical equations (4.5) is a function which is nonanalytic at the origin, we do not expect solutions for higher electric multipoles in closed form. The set of two complex differential equations of second order therefore was transformed into a set of eight real differential equations of first order which was solved numerically by Hamming's modified predictor-corrector method. Equations (4.7) and (4.8) provide six boundary values at the nuclear surface and the four unknown quantities x_l, W, i.e., real and imaginary parts of the eigenfrequency and tangential component of the fluid velocity at the surface, were computed with a four-parameter search under the constraint that radial and tangential fluid velocity components vanish at the origin.

The complex solution for the 1^- squeezing mode is also included in Fig. 6. This mode, being a superposition of translational and compressional motion, is not spurious. Its width comes out to be very small and even negative. This is quite understandable on grounds that the damping force (2.26) derived from the long-mean-free-path damping mechanism essentially is a radial force, whereas squeezing motion is mainly tangential. Similarly, the widths of the 3^- and 4^+ vibrational modes turn

out to become negative for large values of η. They are therefore not shown. The width of the 2^+ octupole vibration, however, is of the correct order of magnitude. The occurrence of negative widths shows that the assumption of specular reflections wherein the tangential component of momentum is always conserved[31] no longer gives a valid picture of the damping mechanism and, hence, the simple piston model with no tangential damping stresses becomes inadequate.

C. Magnetic modes

Vibrational modes of abnormal parity, 1^+, $2^-, \ldots$, also called magnetic or twist modes, were put forward by Holzwarth and Eckart[4] as solutions of the long-mean-free-path fluid dynamical equations. They let the nuclear surface stay spherical and the radial velocity vanish everywhere. According to Eq. (2.26), the damping force vanishes identically and, hence, these modes are not damped by our damping mechanism. For the solution of the Euler equations of motion we therefore refer to previous work.[16–18]

V. SUMMARY AND OUTLOOK

The first part of this paper was concerned with the derivation of a damping stress tensor from the Boltzmann equation. We employed the model of a spherical Fermi gas nucleus whose solid wall breathes harmonically. The collision term is treated in first order in the perturbation of the distribution function arising from specular reflection of the particles from the wall. This is equivalent to the assumption of a very large mean free collision time (or mean free path) in the interior.

This damping stress results in a damping force which was then assumed to hold for variations of arbitrary multipolarity of the free nuclear surface. Energies and widths of low lying collective resonances were then calculated as eigenfrequencies of a vibrating nucleus under the influence of surface tension, the Coulomb potential, and the damping force. Energies and widths of the high-lying isoscalar giant resonances, on the other hand, were calculated as eigenfrequencies of an elastic nucleus with damping force, the elastic behavior resulting from the conservative part of the pressure tensor in the long-mean-free-path limit.

The model itself has no adjustable parameters. However, in order to study the influence of damping on the motion we varied the strength of the damping force and found maximum damping of the hydrodynamic vibrations if the particle frequency is approximately in resonance with the wall frequency. A comparison of the theoretical results obtained with the Fermi gas values with the experimetal widths showed reasonable agreement, thereby implying that the total width is to be identified with the spreading width only.

Many an assumption entering the model can be relaxed in future work: the derivation of the stress tensor from radial motion only, i.e., neglection of any tangential dissipation mechanism; the assumption of a sharp surface; the assumption of very long mean-free-path in the interior; the neglection of higher than second moment of the Vlasov equation in the pressure tensor; the Fermi gas assumption; and the linearization of the fluid dynamical equations.

All models considered above have dimensionless frequencies $x_l \approx 2 \cdots 4.5$. Phases of the disturbed distribution function (2.10) hence are of the order of

$$\frac{R_0 \mathrm{Re}(\Omega_l)}{v_F} = \frac{x_l}{\sqrt{5}} \approx 1 \cdots 2 \,. \tag{5.1}$$

The argument of a rapid oscillation is therefore only applicable for large multipole numbers. This, however, is consistent with here neglecting terms in the conservative part of the pressure tensor which are proportional to x_l^{-2}, cf. Ref. 18.

ACKNOWLEDGMENTS

R.W.H. would like to thank the members of the Nuclear Science Division, Lawrence Berkeley Laboratory, for the warm hospitality extended to him. He acknowledges fruitful discussions with Dr. W. J. Swiatecki. G. G. would like to thank the Alexander von Humboldt foundation for a fellowship. He also thanks Prof. G. Süssmann and the members of the Sektion Physik, Universität München, for the warm hospitality extended to him. This work was supported in part by Deutsche Forschungsgemeinschaft, Bundesministerium für Forschung und Technologie, Alexander von Humboldt foundation, and USDOE Contract W-7405-ENG-48.

*Work by R. W. H. was partly done at Sektion Physik, Universität München, D-8046 Garching, West Germany; Present address: Institut Laue-Langevin, F-38042 Grenoble, France.

[1]G. F. Bertsch, Ann. Phys. (N.Y.) 86, 138 (1974).

[2]G. F. Bertsch, Nucl. Phys. A249, 253 (1975).

[3]G. F. Bertsch, *Les Houches Lectures 1977, session XXX* (North-Holland, Amsterdam, 1978), Vol. 1, p. 175.

[4]G. Holzwarth and G. Eckart, Z. Phys. A 283, 219 (1977).

[5]G. Holzwarth and G. Eckart, Z. Phys. A 284, 291 (1978).

[6]H. Sagawa and G. Holzwarth, Prog. Theor. Phys. 59, 1213 (1978).

[7]G. Holzwarth and G. Eckart, Nucl. Phys. A325, 1 (1979).

[8]G. Eckart, G. Holzwarth, and J. P. Providencia, Nucl. Phys. A364, 1 (1981).

[9]T. Yukawa and G. Holzwarth, Nucl. Phys. A364, 29 (1981).

[10]N. Azziz, J. C. Palathingal, and R. Méndez-Plácido, Phys. Rev. C 13, 1702 (1976).

[11]C. Y. Wong and J. A. MacDonald, Phys. Rev. C 16, 1196 (1977).

[12]J. Winter, private communication.

[13]J. Winter, *Proceedings of the Workshop on Semiclassical Methods in Nuclear Physics, Grenoble, 1981* (Institut Laue-Langevin Report, 1981), No. 15.

[14]J. R. Nix and A. J. Sierk, Phys. Rev. C 21, 396 (1980).

[15]E. E. Balbutsev, R. Dymarz, I. N. Mikhailov, and Z. Vaishvila, Phys. Lett. 105B, 84 (1981).

[16]R. W. Hasse, A. Lumbroso, and G. Ghosh, *Proceedings of the International Workshop IX on Gross Properties of Nuclei and Nuclear Excitations, Hirschegg, 1981,* edited by H. Feldmeier (Technische Hochschule, Darmstadt, 1981), p. 44.

[17]R. W. Hasse and G. Ghosh, *Proceedings of the Workshop on Semiclassical Methods in Nuclear Physics, Grenoble, 1981* (Institut Laue-Langevin Report, 1981), No. 16.

[18]R. W. Hasse, G. Ghosh, J. Winter, and A. Lumbroso, Phys. Rev. C 25, 2771 (1981).

[19]C. Y. Wong and N. Azziz, Phys. Rev. C 24, 2290 (1981).

[20]H. H. K. Tang and C. Y. Wong, J. Phys. A 7, 1038 (1974).

[21]R. W. Hasse, Ann. Phys. (N.Y.) 93, 68 (1975).

[22]N. Auerbach and A. Yeverechyahu, Ann. Phys. (N.Y.) 95, 35 (1975).

[23]P. Nerud, and R. W. Hasse, J. Phys. G 4, L51 (1978).

[24]L. D. Landau and E. M. Lifshitz, *Theory of Elasticity* (Pergamon, New York, 1959), Chap. 31.

[25]J. Blocki, Y. Boneh, J. R. Nix, J. Randrup, M. Robel, A. J. Sierk, and W. J. Swiatecki, Ann. Phys. (N.Y.) 113, 330 (1978).

[26]G. Wegmann, *Proceedings of the International Workshop III on Gross Properties of Nuclei and Nuclear Excitations, Hirschegg, 1975,* edited by W. D. Myers (Technische Hochschule, Darmstadt, 1975), p. 28.

[27]R. W. Hasse, J. Phys. G 5, L101 (1979).

[28]W. D. Myers, W. J. Swiatecki, T. Kodama, L. J. El-Jaick, and E. R. Hilf, Phys. Rev. C 15, 2032 (1977).

[29]P. Schuck and J. Winter, Phys. Lett. (to be published).

[30]A. A. Abrikosov and I. M. Khalatnikov, Usp. Fiz. Nauk 56, 177 (1958) [Sov. Phys.—Usp. 1, 68 (1958)].

[31]I. L. Bekarevich and I. M. Khalatnikov, Zh. Eksp. Teor. Fiz. 39, 1699 (1960) [Sov. Phys.—JETP 12, 1187 (1961)].

[32]R. W. Hasse, Rep. Prog. Phys. 41, 1027 (1978).

[33]K. Huang, *Statistical Mechanics* (Wiley, New York, 1963), Chap. 3.5.

[34]According to L. D. Landau and E. M. Lifshitz, *Fluid Dynamics* (Addison-Wesley, Reading, 1959) stress is defined as a negative traceless part of the pressure tensor.

[35]N. Bohr and J. A. Wheeler, Phys. Rev. 56, 426 (1939).

[36]J. M. Moss, D. H. Youngblood, C. M. Rozsa, D. R. Brown, and J. D. Bronson, Phys. Rev. Lett. 37, 816 (1976).

[37]J. M. Moss, D. R. Brown, D. H. Youngblood, C. M. Rozsa, and J. D. Bronson, Phys. Rev. C 18, 741 (1978).

[38]F. Bertrand, *Proceedings of the International Conference on Nuclear Physics, Berkeley, 1980,* edited by R. M. Diamond and J. O. Rasmussen (North-Holland, Amsterdam, 1981), p. 129c.

[39]J. Speth and A. van der Woude, Rep. Prog. Phys. 44, 179 (1981).